PAPER

3D hydrogel-based microwell arrays as a tumor microenvironment model to study breast cancer growth

To cite this article: John Casey *et al* 2017 *Biomed. Mater.* **12** 025009

Biomedical Materials

PAPER

3D hydrogel-based microwell arrays as a tumor microenvironment model to study breast cancer growth

John Casey[1], **Xiaoshan Yue**[2], **Trung Dung Nguyen**[2], **Aylin Acun**[3], **Victoria R Zellmer**[4,5], **Siyuan Zhang**[4,5] and **Pinar Zorlutuna**[2,3,5]

[1] Department of Chemical and Biomolecular Engineering, University of Notre Dame, Notre Dame, IN 46556, United States of America
[2] Department of Aerospace and Mechanical Engineering, University of Notre Dame, Notre Dame, IN 46556, United States of America
[3] Bioengineering Graduate Program, University of Notre Dame, Notre Dame, IN 46556, United States of America
[4] Department of Biological Sciences, University of Notre Dame, Notre Dame, IN 46556, United States of America
[5] Harper Cancer Research Institute, University of Notre Dame, Notre Dame, IN 46556, United States of America

E-mail: Pinar.Zorlutuna.1@nd.edu

RECEIVED
11 November 2016

REVISED
30 January 2017

ACCEPTED FOR PUBLICATION
1 February 2017

PUBLISHED
15 March 2017

Keywords: breast cancer, microwell array, polyethylene glycol acrylate, gelatin methacrylate, tumor microenvironment

Abstract

The tumor microenvironment (TME) is distinctly heterogeneous and is involved in tumor growth, metastasis, and drug resistance. Mimicking this diverse microenvironment is essential for understanding tumor growth and metastasis. Despite the substantial scientific progress made with traditional cell culture methods, microfabricated three-dimensional (3D) cell cultures that can be precisely controlled to mimic the changes occur in the TME over tumor progression are necessary for simulating organ-specific TME *in vitro*. In this research, to simulate the breast cancer TME, microwell arrays of defined geometry and dimensions were fabricated using photo-reactive hydrogels for a cancer cell line and primary explant tissue culture. Microwell arrays fabricated from 4-arm polyethylene glycol acrylate and methacrylated gelatin with different degrees of methacrylation for controlled cell–matrix interactions and tunable stiffness were used to create a platform for studying the effects of distinct hydrogel compositions and stiffness on tumor formation. Using these microwell arrays, size-controlled spheroids of human breast cancer cell line HCC1806 were formed and the cell attachment properties, viability, metabolic activity, and migration levels of these spheroids were examined. In addition, primary mammary organoid tissues explanted from mice were successfully cultured in these hydrogel-based microwell arrays and the organoid morphology and viability, as well as organoid branching were studied. The microwell array platform developed and characterized in this study could be useful for generating a tissue-specific TME for *in vitro* high throughput studies of breast cancer development and progression as well as in drug screening studies for breast cancer treatment.

1. Introduction

Tumor growth and progression depends on its surrounding microenvironment. It has become increasingly recognized that tumor microenvironment (TME) factors are among the major regulators of tumor growth and metastasis [1–3]. The extracellular matrix (ECM) is one of the major components of TME, whose properties, such as stiffness, porosity, structure, and composition, play important roles in tumor initiation and progression [4–6]. Mounting evidence suggests that breast tissue stiffness is able to affect breast tumorigenesis, progression, and metastasis [7, 8]. *In vitro* studies showed that breast tissue transformation is accompanied by collagen crosslinking, which modulates tissue fibrosis and stiffness. The stiffened matrix has been shown to increase focal adhesions and promote breast malignancy [9]. Other studies suggested that the increased stroma and matrix stiffness, as well as elevated cytoskeletal tension caused increased tumor rigidity and enhanced ERK activation, and promoted tumor cell proliferation [10].

To study the effects of TME on cell behavior, substrate stiffness and ECM compositions can be manipulated by tuning the biochemical and biophysical properties of synthetic materials. One widely used material for such purposes is polyacrylamide gel. By controlling the concentration of acrylamide and its

ratio to bisacrylamide, the stiffness of generated gels can range from 200 Pa to 120 kPa, which provides a range that covers most native tissue stiffness [11, 12]. However, because of the cytotoxicity of the non-polymerized gel solution, the polyacrylamide gels were mostly used for 2D studies [10, 13]. In addition to the approaches with 2D cultures, efforts were made for developing 3D culture models, which enable the study of complex 3D interactions in addition to its advantage of having potentially tunable TME parameters [14–16]. In particular, microfabricated 3D cultures that take the ECM composition, stiffness and geometry into account can be used to imitate the native TME more precisely. A 3D cell culture material that has been extensively explored for cancer studies is commercially available Matrigel. Matrigel is ECM extracted from the Engelbreth–Holm–Swarm mouse sarcoma and could form hydrogel structures when heated to 37 °C. However, the components in Matrigel are poorly characterized and the control over its biochemical and biophysical properties is very limited. In addition, it is not readily castable into defined shapes or geometries, in other words, it is hard to create controlled 3D structures using Matrigel through microfabrication approaches. One way to gain more precise control over the 3D microenvironment geometry and stiffness is to use photo-reactive hydrogels. It is possible to methacrylate the macromolecules within the ECM and render it photocrosslinkable to attain stable hydrogels with defined microstructures [17]. By controlling the methacrylation degrees and the UV exposure time, the stiffness of these hydrogels can be easily controlled to account for different stiffness levels of *in vivo* ECMs [18, 19]. For example, photocrosslinkable hydrogels made using methacrylated collagen [20, 21], elastin [22], and gelatin [19] were reported for their suitability for use in cell culture. Synthetic polymers such as polyethylene glycol (PEG) have also been extensively used with methacrylation modification to model different ECM stiffnesses for cell culture [23, 24]. However, in most of these studies cells were cultured either on the surface of these hydrogels or by encapsulating single cells randomly within the hydrogels. 3D tissue culture models that promote formation of structures resembling that of tumor spheroids with controllable size and with a surrounding matrix with tunable composition and stiffness could provide more precise control over the TME, and are essential for understanding the effects of TME on tumor initiation, progression, and metastasis.

In this study, we microfabricated hydrogel-based microwell arrays as a versatile platform to study breast cancer using either a human breast cancer cell line or mouse primary mammary organoids. We used two different compositions of hydrogels: a synthetic hydrogel, 4-arm PEG acrylate (Molecular Weight: 20 kDa), which does not allow for cell-ECM interactions, and a natural hydrogel, methacrylated gelatin (GelMA), which cells can adhere to and remodel, as a platform to study the influence of cell-ECM interactions on tumor progression. Furthermore, we used two types of GelMA with different methacrylation degrees, thus different stiffnesses (referred to as GelMA-Low for lower methacrylation degree and GelMA-High for higher methacrylation degree) as a means to control the stiffness of the TME.

2. Methods

2.1. GelMA synthesis and characterization

GelMA was synthesized as reported previously [19]. Briefly, methacrylic anhydride (MA, Sigma) was added to 10% (w/v) gelatin (porcine skin, type A, Sigma) in phosphate buffered saline (PBS, Invitrogen), reaction was run at 60 °C for 3 h with vigorous stirring, and then dialyzed with Spectra/Por Molecularporous Membrane Tubing (12–14 kDa, Spectrum Laboratories, Inc.) against PBS at 40 °C–50 °C for 7 days, followed by lyophilization. The degree of methacrylation was confirmed by ^{1}H NMR as described previously [22].

2.2. Microwell fabrication and characterization

The 3-(trimethoxysilyl)propyl methacrylate (TMSPMA, Sigma Aldrich)-coated glass slides were prepared by treating glass slides with 2.8 M NaOH overnight followed by washing with 100% ethanol and baking at 80 °C for one hour. The treated glass slides were then evenly coated with TMSPMA for 30 min and baked at 80 °C overnight. After washing with 100% ethanol and air-drying, the glass slides were baked again at 80 °C for one hour before being ready for use. The polydimethylsiloxane (PDMS) stamps were prepared in a similar method as described before [25], by peeling the cured silicone elastomer base and curing agent (Sylgard 184, Dow Corning) mixture (with 10:1 ratio) from a silicon wafer containing protruding columns with diameters of 300 μm and a spacing of 1000 μm between each column. 4-arm PEG 20 kDa acrylate (JenKem Technology) and GelMA photocrosslinked hydrogels were prepared using 10% w/v PEG/PBS solutions or 5% GelMA/PBS solutions each containing 0.1% w/v 2-hydroxy-1-(4-(hydroxyethoxy) phenyl)-2-methyl-1-propanone (Irgacure 2959, BASF Corporation) as photoinitiator. Each hydrogel-based microwell array was fabricated using 16.5 μl of hydrogel precursor solution sandwiched between a TMSPMA-coated glass slide and the PDMS stamp with microwell patterns, separated by 250 μm spacers. Crosslinking was initiated by exposing to 6.9 mW cm^{-2} UV light for 30 s for the PEG-based precursor and 25 s for the GelMA-based precursors. Interwell and intrawell swelling ratios were determined on different time points by measuring the distances between nearest edges of two microwells and the microwell diameters, respectively, and compared against their respective initial state (day 0). Stiffness of

the hydrogel-based microwell arrays were measured using a nanoindenter (Piuma Chiaro, Optics11, Amsterdam, The Netherlands). The indentation probe used had a spring constant and tip diameter of approximately 0.261 N m^{-1} and 16 μm, respectively. Before testing, the sensitivity calibration of cantilever was conducted by indenting a glass slide. Each sample was tested at 10 different locations, 5 of which conducted near and the other 5 far away from the microwells, with 5 repetitions at each location with a loading velocity of 2 μm s^{-1}. A MATLAB code (MathWorks, Inc.) was developed to determine contact points between the probe and samples and to identify elastic moduli of hydrogel-based microwell arrays using Hertz contact model [26–28]. Note that the hydrogels were assumed to be incompressible (i.e. Poisson's ratio is 0.5).

2.3. Cell and organoid culturing and seeding

Human breast cancer cell line HCC1806 was cultured in RPMI 1640 (Gibco) with 10% fetal bovine serum (FBS, Hyclone) and 1% penicillin–streptomycin (P/S, Gibco) at 37 °C with 5% CO_2. Organoids were collected from the fourth inguinal mammary glands of female FVB mice as previously reported with minor modifications [29]. All experiments were conducted in accordance to the Institutional Animal Care and Use Committee of the University of Notre Dame. Briefly, mammary glands were minced and treated with collagenase for 3 h and centrifuged to remove top fatty layer. DNase was added to the pellet for 2–5 min followed by dilution in DMEM/F12 (Gibco) media and a centrifuging step to remove single cells from organoids. For seeding on hydrogel-based microwell arrays, HCC1806 cells were resuspended in RPMI (Gibco) media to a concentration of 10^6 cells ml^{-1}, and 30 μl of suspension was pipetted onto each microwell array. The organoids were resuspended in DMEM/F12 media at a concentration of 5000 organoids ml^{-1}, and 40 μl of the suspension was pipetted onto each microwell array. After incubation for 5 min, the hydrogel-based microwell arrays were tilted at a 15° angle to gently wash away the excess cells or organoids out of the microwells with 300–400 μl of media. Washing was repeated twice for each hydrogel-based microwell array sample. Each hydrogel-based microwell array was then covered with RPMI 1640 with 10% FBS and 1% P/S for HCC1806 cells, or DMEM/F12 media supplemented with 1% P/S and 1% insulin/transferrin/sodium selenite (ITS, Gibco) for organoids for cell culture.

2.4. Cell viability, proliferation, and spreading/migration test

Cell viability was measured on days 1 and 5 of the cell culture using Live/Dead assay kit (Invitrogen) according to manufacturer's instructions. Briefly, hydrogel-based microwell arrays with cells were incubated with PBS containing 0.5 μl ml^{-1} of calcein AM and 2 μl ml^{-1} of ethidium homodimer-1 (EthD-1) at 37 °C for 30 min. Cell aggregates inside microwells were visualized with an inverted fluorescence microscope (Zeiss Axio Observer.Z1) for live (green) and dead (red) cells. For each cell aggregate, z-stack images were taken throughout the aggregate with a stepping distance of 5 μm, and compiled into one image to represent a single aggregate. Live and dead cell numbers were recorded by counting cells with green or red fluorescence using ImageJ software (version 1.50i, National Institutes of Health). Cell viability was calculated based on the fluorescence intensity. The cellular metabolic activity was determined using alamarBlue assay (Thermofisher). Hydrogel-based microwell arrays containing cell aggregates were incubated in alamarBlue reagent diluted at a ratio of 1:10 in serum-free media at 37 °C for 4 h. The fluorescence intensity of the alamarBlue reagent was measured at 590 nm using a microplate reader (1420 Multilabel Counter, Perkin Elmer). Percent reductions of the reagent, which correlates to the cellular metabolic activities, were calculated for each of the hydrogel materials. Three measurements were taken from each of six microwell arrays for both GelMA-High and GelMA-Low hydrogels (a total of 18 measurements for each type of hydrogel). Similarly, three measurements were taken from each of four PEG 20 kDa microwell arrays (a total of 12 measurements for PEG 20 kDa arrays). Percent reduction was calculated from each of these measurements. The results were normalized to the mean of three blank samples, containing only the alamarBlue reagent with unseeded microwells. Cell spreading and migration into hydrogels was quantified by measuring the area and the diameter of cell aggregates on days 1 and 5 of culture using ImageJ software. Five sample microwells were selected from each of the six hydrogel-based microwell arrays for all three hydrogel materials ($n = 30$ for each hydrogel material). The diameters of the aggregates were measured with the furthest horizontal distance across the aggregate. The area of each spheroid was measured by tracing along their perimeters. MATLAB was used to fit the aggregate areas into a built-in *ksdensity* function to create the probability density function of aggregate areas for each hydrogel-based microwell array, to show the distribution of cell aggregate areas in each hydrogel material.

2.5. Statistical analysis

Data was analyzed for statistical significance using one-way ANOVA test or Student's t-test ($^{*}p < 0.01$, $^{**}p < 0.001$, $^{***}p < 0.0001$). Error bars represent mean ± standard deviation (SD).

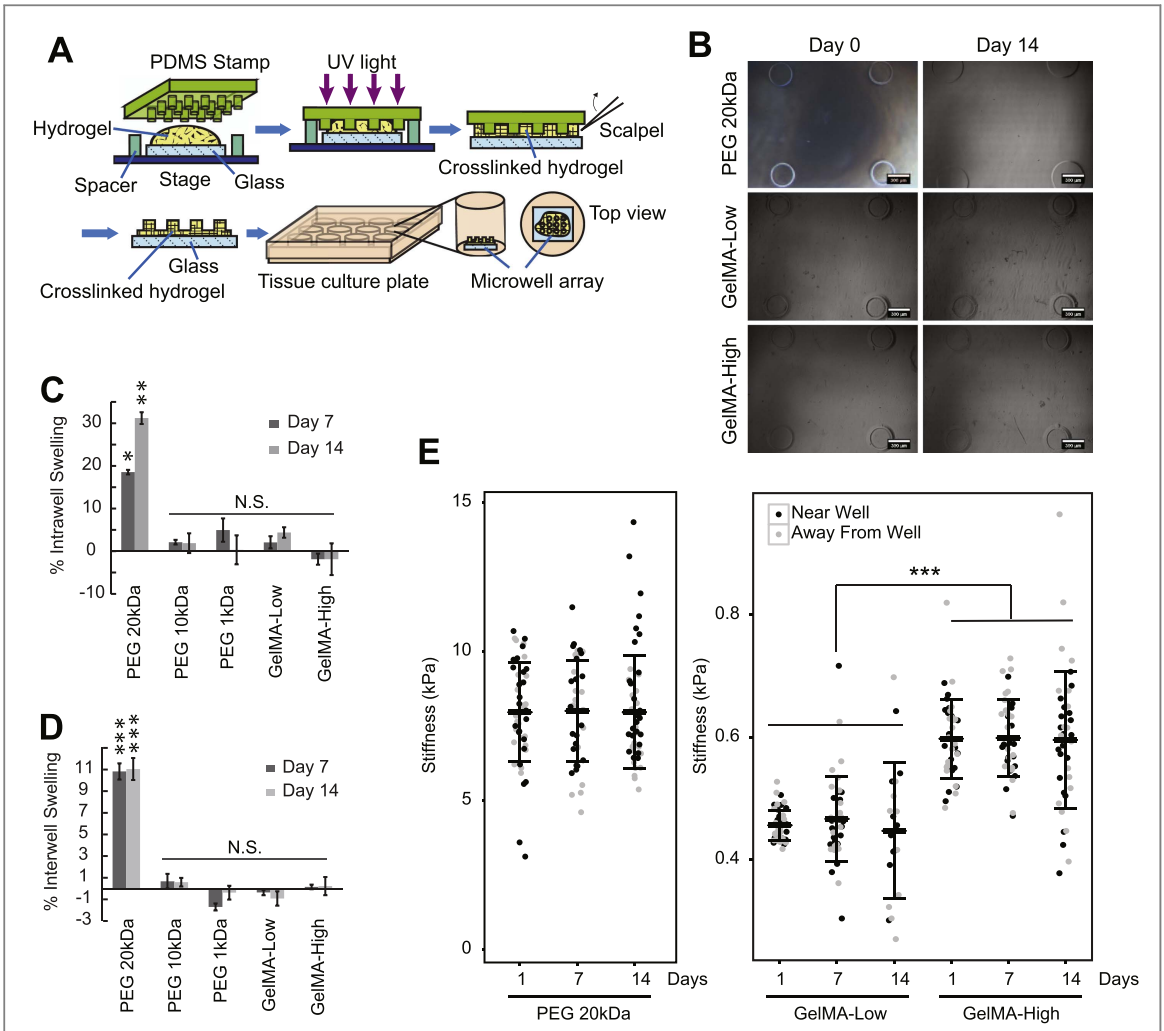

Figure 1. Microwell fabrication and characterization. (a) Schematic of the microwell fabrication process using PEG 20 kDa, GelMA-Low and GelMA-High hydrogels. (b) Brightfield images of the microwell arrays on days 0 and 14 (scale bar = 300 μm). (c) Intrawell and (d) interwell swelling ratios calculated compared to microwell array dimensions of each material on day 0. PEG 10 kDa and PEG 1 kDa were used as controls for PEG 20 kDa in swelling studies. (e) Stiffness of PEG 20 kDa, GelMA-Low and GelMA-High microwell arrays through nanoindentation measurements. Three microwell arrays were tracked over the course of 14 days with five locations tested near microwells and five locations far away from microwells ($n = 3$). Data is presented as mean $\pm$ SD. $^{*}p < 0.01$, $^{**}p < 0.001$, $^{***}p < 0.0001$, N.S.: no statistically significant differences.

3. Results

3.1. Characterization of the microwell arrays

Microwell arrays prepared using PEG with different molecular weights and GelMA with different methacrylation degrees were tested for their long-term stability after being fabricated as illustrated in figure 1(a). PEG is a non-biofouling material that possesses favorable hydration properties similar to the native ECM. Since PEG has no natural biological motifs, cells cannot adhere to or degrade it [8, 24]. On the other hand, GelMA is methacrylated gelatin and contains cell-binding and cell-degradable sequences, which allows for cell adhesion and degradation [8, 24]. We used three types of PEG (with molecular weights of 1 kDa, 10 kDa, and 20 kDa) and two types of GelMA (GelMA-Low with methacrylation degree of 28% and GelMA-High with methacrylation degree of 45%, data not shown) to fabricate hydrogel-based microwell arrays with microwell depth of 120 μm, microwell diameter of 300 μm, and microwell spacing of 1 mm (measured from the perimeter edge of one well to the perimeter edge of the adjacent well).

The brightfield images of microwell arrays were shown in figure 1(b). We examined the swelling properties of the microwell arrays for intrawell and interwell swelling on days 1, 7 and 14 in order to assess the microwell stability for long-term culture (two independent experiments, $n = 3$ for each). Over 14 days, PEG with 20 kDa molecular weight exhibited intrawell swelling of 18% on day 7 and 31.2% on day 14. This was the largest swelling observed amongst the five different hydrogel-based microwell arrays we tested in this study. All other microwell arrays exhibited minimal swelling of less than $\pm$5% of the original microwell dimensions (figure 1(c)). In addition, PEG 20 kDa exhibited the highest degree of interwell swelling around 11% on both days 7 and 14 (figure 1(d)). Although PEG 20 kDa showed the highest degree of swelling, the microwell arrays were intact without

degradation for 14 days of cell culture conditions. Since PEG 20 kDa is the softest and most cell compatible material [30] relative to other PEG-based hydrogel-based microwell arrays we tested (PEG 10 kDa and PEG 1 kDa), we chose PEG 20 kDa for future experiments despite of its swelling properties.

Next, we measured the stiffness of the microwells fabricated from PEG and GelMA hydrogels through nanoindentation measurements at various locations (10 different locations per microwell array, three measurements at each location, and on three different microwell arrays per time point) on the microwell array surface. Unseeded microwell arrays were kept in PBS under cell culture conditions and the measurements were performed on days 1, 7, and 14 (figure 1(e)). The elastic modulus was uniform throughout the microwell arrays with no significant differences between the measurements taken near the wells and far from them, and was around 8 kPa for PEG 20 kDa microwell arrays, 460 Pa for GelMA-Low microwell arrays, and 600 Pa for GelMA-High microwell arrays, which remained constant throughout the 14 day cell culture period. By controlling the methacrylation degree of GelMA and the UV treatment duration, the stiffness of GelMA hydrogels we tested ranged from 260 Pa to 3.3 kPa (data not shown), which is relevant to the range of various *in vivo* stiffness conditions for both normal and cancerous breast tissues and their ECMs [9, 10]. In addition, increasing the GelMA concentration to 10% instead of the 5% used in this study can further increase the stiffness to tens of kPa range [19].

3.2. Cell viability and proliferation

HCC1806 cells were seeded on microwell arrays fabricated using PEG 20 kDa, GelMA-Low and GelMA-High, as shown in figure 2(a). Brightfield as well as fluorescent images after staining the cells with Live/Dead stain were recorded to show the distribution of the cell seeded microwell arrays and to visualize the 3D structure of the cells cultured in the microwells. In all three types of microwell arrays, HCC1806 cells formed compact spheroids in each microwell, while the size of the cell aggregates within the PEG 20 kDa microwells appeared smaller than the cell aggregates within the GelMA-Low and GelMA-High microwells (figure 2(b)).

The viabilities of HCC1806 cells in PEG 20 kDa, GelMA-Low, and GelMA-High microwell arrays were assessed on days 1 and 5 of culture using Live/Dead assay (figure 3(a)). There was no significant difference in cell viability among the top, middle, and bottom *z*-positions in the cell aggregates in all three hydrogel materials, and as such, the cell viabilities for each group is given as average of all the layers from the entire cell aggregate. HCC1806 cells cultured in PEG 20 kDa, GelMA-Low, and GelMA-High microwells all showed high viabilities (figure 3(b)) with similar live cell count per microwell array (figure 3(c)). There were no significant differences in cell viability or live cell counts among the microwell arrays fabricated using the three different types of hydrogels.

We also examined the metabolic activities of HCC1806 cells cultured on microwell arrays fabricated from different types of hydrogels using an alamarBlue assay (figure 3(d)). Cell aggregates cultured in PEG 20 kDa microwells showed lowest reduction ratio of the alamarBlue reagent (31.8% on day 5), indicating the lowest metabolic activity and thus slowest growth rate. Cell aggregates cultured in GelMA-Low and GelMA-High microwells both showed higher metabolic activity, with alamarBlue reagent reduction ratio of 70.2% for GelMA-High and 59.3% for GelMA-Low on day 5. Cell aggregates within GelMA-High, had a faster metabolic growth rate than cell aggregates within GelMA-Low, increasing from 22.2% reduction to 56.8% reduction from days 1 to 3 in culture. Although HCC1806 cells in GelMA-Low and GelMA-High microwells had different metabolic growth rates, they reached similar activity levels by day 5 in culture suggesting a potential growth limiting effect due to restrictions imposed by the size of the microwells.

3.3. Cell migration

To study the cell migration out from the cell aggregates over time in culture, the change in aggregate areas were measured on days 1 and 5 using ImageJ software (figure 4(a)). Five microwells from six samples of each hydrogel material were analyzed, for a total of 30 data points for each type of microwell array. An estimated probability density function of cell aggregate areas was fitted to the data obtained for each hydrogel material using MATLAB (figure 4(b)). Cell aggregates in microwells of both GelMA-Low and GelMA-High had narrow area distributions at day 1 but over time, the distribution widened and the average aggregate area increased by day 5. In GelMA-Low microwells the average spheroid area increased from 0.105 ± 0.009 to $0.131 \pm 0.030\ mm^2$ from days 1 to 5 in culture. In GelMA-High microwells the average spheroid area increased from 0.101 ± 0.007 to $0.124 \pm 0.027\ mm^2$ from days 1 to 5 in culture. However the average spheroid area in PEG 20 kDa microwells decreased from $0.057 \pm 0.013\ mm^2$ to $0.047 \pm 0.013\ mm^2$ from days 1 to 5 in culture as the cell aggregates condensed into dense spheroids likely due to the lack of cell-ECM adhesion in PEG 20 kDa microwells. The distribution of spheroid areas in the PEG 20 kDa microwells was narrower than those of the GelMA microwells on both days 1 and 5, indicating a lower degree of variation within the cell aggregate growth in PEG 20 kDa microwells. Aggregate growth was more diverse within the microwell arrays made from GelMA hydrogels. Cell spreading into the interwell spaces was pronounced in the GelMA hydrogel-based microwell arrays as evident by spreading cells that were observed

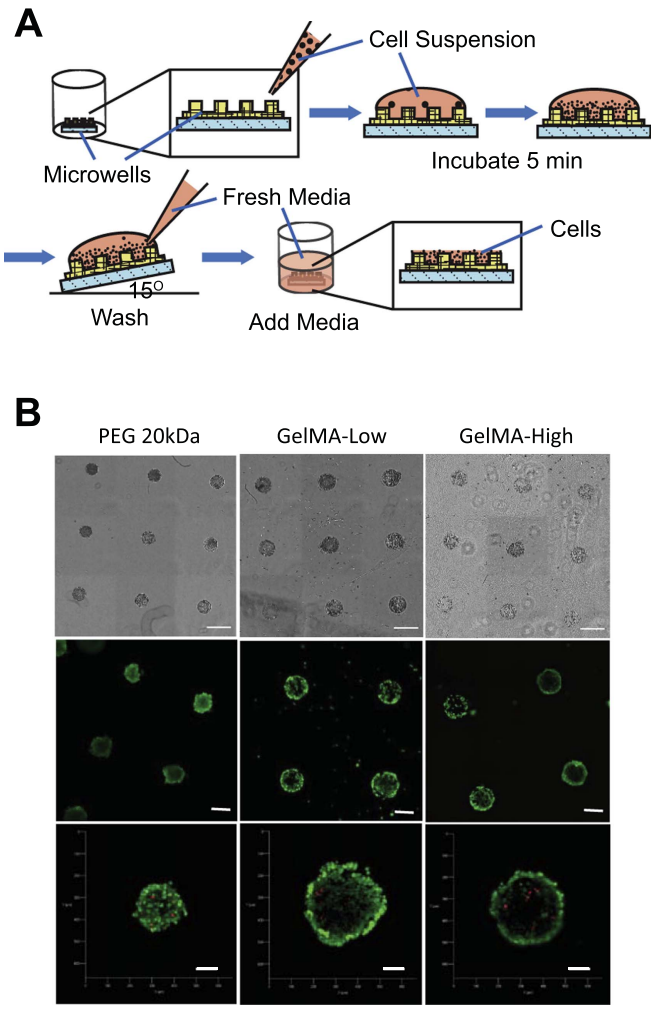

Figure 2. Cell seeding in microwell arrays fabricated using PEG 20 kDa, GelMA-Low and GelMA-High. (a) Schematic of the cell seeding process. (b) Brightfield (top row, scale bar = 500 μm) and fluorescence microscopy (middle row, scale bar = 200 μm and bottom row, scale bar = 100 μm) images on day 1 after cell seeding on to the microwell arrays. For the fluorescence images, Live/Dead stain (green/red, respectively) was used.

at multiple focal planes within the hydrogel throughout the thickness of the microwell array. The cells in the aggregates attached and migrated on the surface of the GelMA microwell arrays due to the cell adhesive properties of GelMA, and degraded and grew into the surrounding gel due to the enzymatically degradable characteristics of GelMA. We also measured the cell aggregate diameters as an additional metric of aggregate growth (figure 4(c)). Spheroids within GelMA-Low and GelMA-High microwells had similar diameters across days 1 and 5. Spheroids within PEG 20 kDa microwells had the narrowest diameters as the cells tended to condense and cluster together (figure 4(d)).

3.4. Organoid viability and proliferation

Primary mouse mammary organoids were seeded in PEG 20 kDa, GelMA-Low, and GelMA-High hydrogel-based microwell arrays and cultured for 7 days. Brightfield images were taken over the 7 day period to document organoid morphologies (figures 5(a) and (b)). Primary mammary organoids exhibited higher growth and spreading rates within both GelMA-Low and GelMA-High microwells, compared to PEG 20 kDa. Within PEG 20 kDa microwells, the organoids condensed and formed aggregates over time, similar to the HCC1806 cells. After 7 days in culture, the mammary organoids within GelMA-Low and GelMA-High microwells grew to fill the size of the microwells and formed 3D structures (figure 5(c)).

Cell viabilities on day 7 were measured using Live/Dead assay (figures 5(c) and (d)). Organoids displayed the lowest viability of 87.9% within PEG 20 kDa microwells, while organoids cultured within GelMA-Low microwells showed the highest viability of 94.7%. No significant differences were shown for cell viabilities between GelMA-Low and GelMA-High microwells. Moreover, organoids exhibited higher cell viability compared to HCC1806 cells for each of the three hydrogel materials tested (figures 3(b) and 5(d)), indicating the potential of all three types of hydrogel-based microwell arrays for long-term organoid culture.

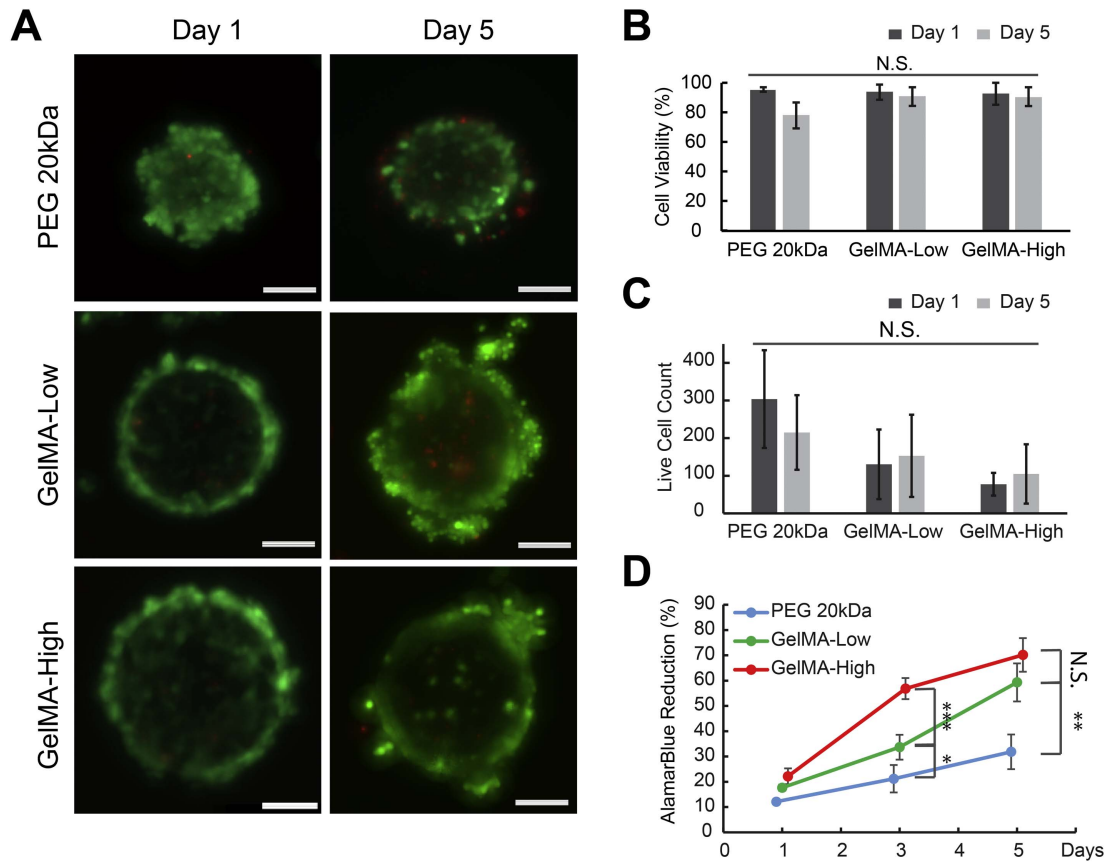

Figure 3. Cancer cell line (HCC1806) viability and proliferation on microwell arrays fabricated using PEG 20 kDa, GelMA-Low and GelMA-High. Live/Dead assay performed on days 1 and 5 of the cell culture and image analysis was carried out using ImageJ software to determine the percent cell viability and total live cell numbers. (a) Fluorescence images of cells stained with Live/Dead stain (green/red, respectively) (scale bar $= 100\ \mu$m). (b) Calculated cell viability rates in the microwell arrays fabricated using PEG 20 kDa, GelMA-Low and GelMA-High over a period of 5 days. (c) Calculated live cell count for each hydrogel material. (d) Cell metabolic activity in the microwell arrays fabricated using PEG 20 kDa, GelMA-Low and GelMA-High over a period of 5 days measured using alamarBlue assay. For the live/dead assay analysis, data were taken from six independent microwell arrays for each hydrogel material, and five microwells were measured in each microwell array ($n = 30$). For the alamarBlue assay analysis, data were taken from six independent GelMA-High microwell samples ($n = 6$), 6 GelMA-Low microwell samples ($n = 6$), and 4 PEG 20 kDa microwell samples ($n = 4$). $^{*}p < 0.01$, $^{**}p < 0.001$, $^{***}p < 0.0001$, N.S.: no statistically significant differences.

4. Discussion

Conventional *in vitro* cell culture methods are routinely used in cancer research to study drug efficacies or for studying cellular responses to various types of stimuli such as changes of nutrient, ion, temperature, or oxygen levels, as well as mechanical pressure or stretching. However, the lack of consideration of an *in vivo* tissue environment such as the ECM and 3D spatial configurations of cells render conventional cell cultures significantly different from the native TME. Lack of accurate *in vitro* 3D representation results in failure to adequately model normal tissue and disease progress, and can be misleading for drug screening before clinical trials [31–34].

By simply growing them on a softer culture surface that promotes cell–cell interactions, breast cancer cells showed dramatic morphological and gene profile differences compared to ones grown on conventional 2D tissue culture plastic [35, 36]. Kenny *et al* compared the morphological phenotypes and gene expression profiles of 25 breast cell lines grown in 2D and 3D cultures, and indicated that cells cultured in 3D microenvironments had significant and reproducible gene expression changes compared to 2D cultures [37]. In addition to their morphology, the culture type can affect the drug response of cancer cells significantly. For example, 3D cultured SKBR-3 breast cancer cells showed significantly more inhibition of their proliferation by trastuzumab treatment compared to 2D cultured cells [38]. The different responses to the treatment might be a result of the differences in protein phosphorylation levels between 2D and 3D cultures, as the author showed that the phosphorylation of human epidermal growth factor receptor 2 (HER2), HER3, and epidermal growth factor receptor levels were upregulated in 3D cultured cells while alpha serine/threonine protein kinase (Akt) signaling pathway was inhibited in 3D cultured cells [39]. In addition, cell polarity, soluble factor diffusion, intercellular interactions, and ECM stiffness were all shown to be distinct in 2D versus 3D cultured cells [39], which might lead to the differences of gene profiles and environmental stimuli responses observed between 2D and 3D

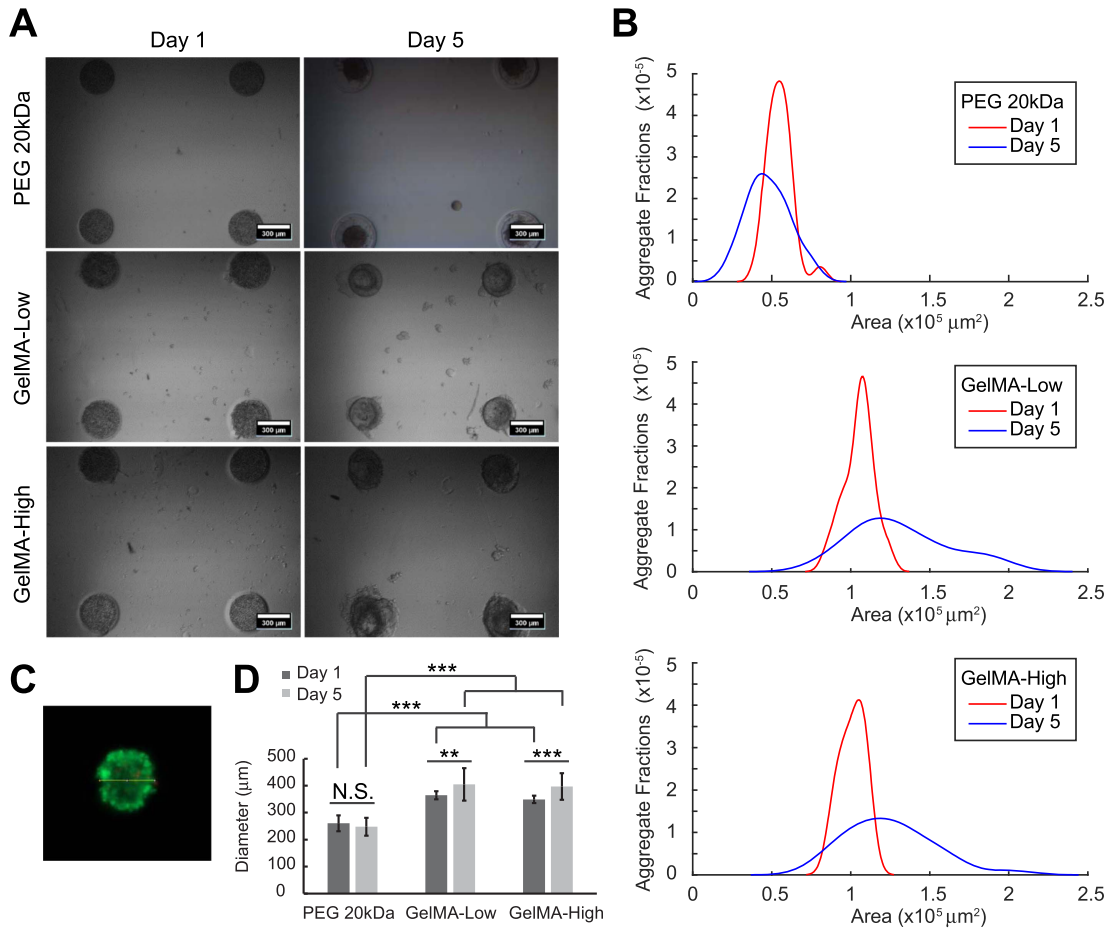

Figure 4. Cancer cell line (HCC1806) aggregate formation, spreading and migration on microwell arrays fabricated using PEG 20 kDa, GelMA-Low and GelMA-High. (a) Brightfield images showing the cell aggregate growth, spreading and migration (scale bar = 300 μm). (b) The distributions of aggregate areas within each type of microwell array were calculated from days 1 and 5 aggregate area measurements using MATLAB. (c) Illustration of measuring diameters of aggregates stained with Calcein AM fluorescent dye (green) using ImageJ software. (d) Quantification of diameter changes of cell aggregates grown on microwell arrays fabricated using PEG 20 kDa, GelMA-Low and GelMA-High hydrogels over a 5 day culture period. Five microwells from 6 independent samples of each hydrogel material were analyzed ($n = 30$ for each hydrogel material). $^{**}p < 0.001$, $^{***}p < 0.0001$, N.S.: no statistically significant differences.

cultured cells. Therefore, to overcome the drawbacks of 2D culture systems, a platform that considers the spatial distribution of cells, as well as the ECM component makeup and stiffness is necessary.

In this study, we have established a 3D hydrogel-based microwell array system with tunable composition and stiffness, which was successfully used for culturing breast cancer cells and primary mammary organoids. We confirmed the viability of the breast cancer cell line HCC1806 and primary organoids from mouse mammary tissues. The growth of HCC1806 cells and the branching of mammary organoids were sustained in 3D hydrogel-based microwell arrays over several days. Hydrogel-based microwell arrays showed suitability for reasonable long-term cell culture without degradation, kept their original stiffness and maintained the microfabricated geometry up to 2 weeks. It is important to note the stiffness and components of the 3D hydrogel-based microwell array platform are adjustable, and additional ECM components, growth factors as well as stromal cells, can be included in the system through encapsulation within the hydrogel during the mild fabrication process to better represent the *in vivo* microenvironment.

Different microwell fabrication methods have emerged in recent years for cell aggregate culture applications. Most of these studies have used microwell arrays fabricated from non-cell interacting materials such as polymethylmethacrylate (PMMA), polystyrene (PS), PDMS, and photopolymerized polyethylene glycol dimethacrylate (PEGDMA) [40–43]. These approaches can homogeneously generate size-controlled cell aggregates, or spheroids that can be used as microtumor models and recapitulate clinical phenotypes of breast cancer for high throughput studies. However, lack of interaction between cells and the ECM could alter the behavior of the cells constituting these spheroids [44–46]. Compared to these approaches, using a hydrogel-based microwell array platform, such as the one described in this study, would allow for generation of tumor cell aggregates or spheroids as well as primary tissue organoids while

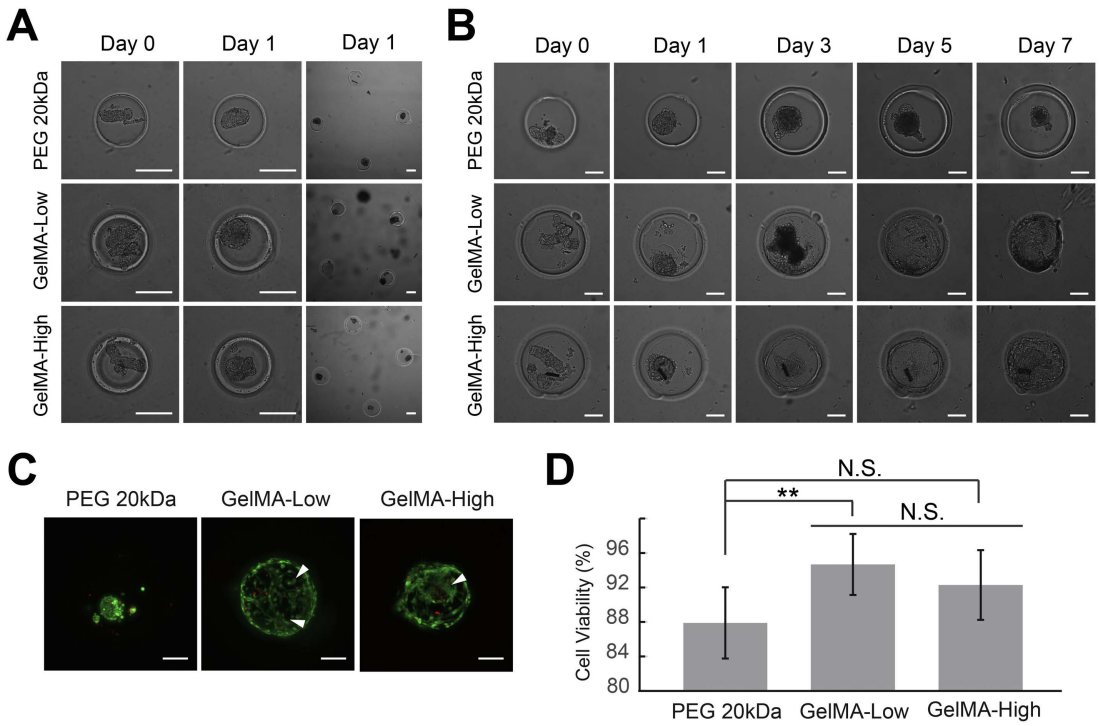

Figure 5. Mouse primary mammary organoid culture in microwell arrays fabricated using PEG and GelMA hydrogels. (a) Brightfield images on day 1 showing both a single microwell and a 2 × 2 grid in the microwell array (scale bar = 200 μm). (b) Brightfield images showing the organoid morphology changes over the course of the 7 day culture period in PEG 20 kDa, GelMA-Low and GelMA-High microwells (scale bar = 100 μm). (c) Live/Dead staining (green/red, respectively) and fluorescence microscopy imaging of mouse primary organoids (scale bar = 100 μm). (d) Quantification of cell viability using ImageJ software. Data were taken from six sample microwells from the PEG-based microwell arrays and seven sample microwells each from GelMA-High and GelMA-Low –based microwell arrays. $^{**}p < 0.001$, N.S.: no statistically significant differences.

maintaining cell-ECM interaction and allowing for tunable TME parameters that could be tailored to satisfy tissue specific design requirements.

Recently, photocrosslinkable hydrogels were used to fabricate hydrogel-based microwell arrays via a two-step approach, which produced stiffer cell-encapsulated regions within the microwells surrounded by an adjacent matrix with lower stiffness [47]. This model was shown to maintain high cell viabilities for both breast cancer cell lines and non-tumorigenic mammary epithelial cells. However, in this system, cells were not forming 3D spheroids, instead each cell in the cell-containing regions was in direct contact with a stiffer matrix surrounded by a softer microwell array. In contrast, in our study, hydrogel-based microwells arrays were fabricated with a homogenous stiffness surrounding each cell aggregate, instead of encapsulating cells in a hydrogel. Both approaches could be valuable for studying different parameters within the TME.

There are studies showing that tumor size is positively correlated with the occurrence of aggressive phenotypes in hormone receptor positive breast cancers [48, 49], and enhanced metastasis with increased spheroid size was observed in *in vitro* studies using 3D tumor spheroids [43]. The diameter measurements of our cell aggregates showed that size of the spheroids formed in the hydrogel-based microwell arrays was dictated by the microwell size and the type of material used to fabricate microwell arrays. The microwell size chosen for our study was based on the average size of mouse mammary organoids, which was tested to be about 150 μm with our organoid isolation protocol. The 300 μm diameter microwells ensures each individual microwell will hold one mammary organoid with space to grow and expand. Interestingly, although they have the same microwell size, the spheroids grown in PEG 20 kDa microwells maintained smaller diameters of 200–300 μm, while spheroids grown in GelMA-High and GelMA-Low filled the majority of the microwell over time and grew to diameters of 300–400 μm indicating the influence of tumor-ECM interactions in tumor spheroid size. These spheroid sizes are suitable to maintain the morphology of breast cancer cells while not enhancing their size-induced metastasis [43]. On the other hand, our results showed that although the cells cultured on GelMA-High hydrogel-based microwell arrays had almost twice as high metabolic activity as those cultured on GelMA-Low hydrogel-based microwell arrays on day 3, they showed no statistical significant differences in their metabolic activities on day 5 (figure 3(d)). This result suggests that the microwell size might impose a growth limiting effect due to its size restriction on the cell aggregates. Furthermore, cell aggregate size measurements showed similar aggregate sizes on GelMA-Low and

GelMA-High microwell arrays on day 5 (figure 4(d)). This finding is supported by a recent study by Thakuri *et al* who showed that the metabolic rates of tumor spheroids were linearly correlated with the spheroid volume [50].

ECM components and stiffness were reported to affect cell behavior such as proliferation and migration [46, 51–53]. Wozniak *et al* reported that breast epithelial cells could sense ECM rigidity through Rho and ROCK mediated contractility [54]. On a softer ECM, ROCK would inhibit Rho activity, which corresponded to inhibited FAK phosphorylation, and caused differentiation in breast epithelial cells. In contrast, cells cultured on stiffer surfaces showed increased proliferation [51]. Mason *et al* showed that both the projected area and perimeter of 3D cultured endothelial cells on collagen gels were significantly increased with higher matrix stiffness [55]. Another study indicated that enhanced stiffness alone could lead to the phenotype changes of mammary cell line MCF10A from non-malignant to malignant, with enhanced migration and increased percentage of invasive cell clusters [50]. Similar phenomena were observed with MCF-7 cells, showing that increased invasiveness was observed on collagen gels with higher stiffness, through prolactin-induced increase in MMP-2 expression [56].

In our study, HCC1806 cells and the organoids cultured on GelMA-High and GelMA-Low did not show significant difference in their spreading and migration into the hydrogel-based microwell arrays. The diameters of cell aggregates on day 1 after seeding were similar for GelMA-High and GelMA-Low hydrogel-based microwell arrays, and over 5 days in culture, the diameters increased to a similar extent in both hydrogel-based microwell arrays. The reason might be that the approximate 30% stiffness difference between GelMA-High and GelMA-Low was not large enough to cause a significant difference in cell migration. On the other hand, although PEG 20 kDa had much higher stiffness (about ten times more compared to GelMA), both the cell aggregates and the organoids reduced in size due to lack of cell-interaction motifs suggesting a more dominant effect of biochemical cell-ECM interactions compared to biophysical ones such as stiffness. On the other hand, there was no significant difference in viabilities of HCC1806 cells seeded on GelMA-High, GelMA-Low, and PEG 20 kDa microwells, indicating that cancer cell viability is not dependent on hydrogel stiffness or on presence of cell-interaction motifs. Whereas, cell proliferation/metabolic activity in GelMA-High was significantly higher compared to GelMA-Low hydrogel-based microwell arrays during the 5 day culture period, indicating that cells in GelMA-High microwells were proliferating more compared to those cultured in GelMA-Low microwells. This result is consistent with previous reports showing that higher stiffness could promote cell proliferation. On the other hand, cells cultured in PEG 20 kDa microwells showed the lowest metabolic activity, potentially due to the lack of interactions with the surrounding hydrogel. Future studies using higher methacrylation degree GelMA for higher stiffness and PEG modified with cell adhesive and MMP-sensitive sequences should be conducted for a more in depth study of these observations.

The results presented in the current manuscript provided a proof-of-concept study to show the capabilities of a hydrogel-based microwell array system with tunable stiffness and cell attachment sequences as a platform for culturing normal and cancerous breast tissues to study the influence of cell-ECM interactions on tumor development. In our future studies we are planning on doing a more detailed analysis on how the ECM stiffness affects the behavior of normal and cancerous breast tissues over a larger range of ECM stiffness.

5. Conclusion

In summary, this study has established a platform using photocrosslinkable hydrogel-based microwell arrays for studying the effect of TME components and stiffness on tumor progress. Both a human breast cancer cell line and mouse mammary organoids exhibited sustained growth and viability over time within the microwell arrays, and showed differences in proliferation, spreading and migration in response to different hydrogel materials and stiffness used. The platform developed here, with tunable hydrogel properties, including biochemical composition, stiffness and microwell size, depth, and spacing distance, as well as possible inclusion of stromal cells through their encapsulation within the microwell array itself, allows precise control over the tissue microenvironment, and could provide a useful tool for tissue-specific cancer research.

Acknowledgments

This work is funded by American Cancer Society IRG-14-195-01 (PZ), Advanced Diagnostics & Therapeutics initiative of University of Notre Dame (PZ), and HCRI Notre Dame Day Pilot Fund (SZ).

References

[1] Joyce J A and Pollard J W 2009 Microenvironmental regulation of metastasis *Nat. Rev. Cancer* **9** 239–52
[2] Meads M B, Gatenby R A and Dalton S W 2009 Environment-mediated drug resistance: a major contributor to minimal residual disease *Nat. Rev. Cancer* **9** 665–74
[3] Quail D F and Joyce J A 2013 Microenvironmental regulation of tumor progression and metastasis *Nat. Med.* **19** 1423–37
[4] Zhu Z R, Agren J, Männistö S, Pietinen P, Eskelinen M, Syrjänen K and Uusitupa M 1995 Fatty acid composition of breast adipose tissue in breast cancer patients and in patients with benign breast disease *Nutrition Cancer* **24** 151–60

[5] Couldrey C, Moitra J, Vinson C, Anver M, Nagashima K and Green J 2002 Adipose tissue: a vital *in vivo* role in mammary gland development but not differentiation *Dev. Dyn.* **223** 459–68

[6] Sun Y and Lodish H F 2010 Adiponectin deficiency promotes tumor growth in mice by reducing macrophage infiltration *PLoS One* **5** e11987

[7] Debnath J, Muthuswamy S K and Brugge J S 2003 Morphogenesis and oncogenesis of MCF-10A mammary epithelial acini grown in three dimensional basement membrane cultures *Methods* **30** 256–68

[8] Lee G Y, Kenny P A, Lee E H and Bissell M J 2007 Three-dimensional culture models of normal and malignant breast epithelial cells *Nat. Methods* **4** 359–65

[9] Levental K R *et al* 2009 Matrix crosslinking forces tumor progression by enhancing integrin signaling *Cell* **139** 891–906

[10] Paszek M J *et al* 2005 Tensional homeostasis and the malignant phenotype *Cancer Cell* **8** 241–54

[11] Solon J, Levental I, Sengupta K, Georges P C and Janmey P A 2007 Fibroblast adaptation and stiffness matching to soft elastic substrates *Biophys. J.* **93** 4453–61

[12] Pathak A and Kumar S 2012 Independent regulation of tumor cell migration by matrix stiffness and confinement *Proc. Natl Acad. Sci. USA* **109** 10334–9

[13] Schmedlen R H, Masters K S and West J L 2002 Photocrosslinkable polyvinyl alcohol hydrogels that can be modified with cell adhesion peptides for use in tissue engineering *Biomaterials* **23** 4325–32

[14] Antoni D, Burckel H, Josset E and Noel G 2015 Three-dimensional cell culture: a breakthrough *in vivo Int. J. Mol. Sci.* **16** 5517–27

[15] Barrila J, Radtke A L, Crabbe A, Sarker S F, Herbst-Kralovetz M M, Ott C M and Nickerson C A 2010 Organotypic 3D cell culture models: using the rotating wall vessel to study host-pathogen interactions *Nat. Rev. Microbiol.* **8** 791–801

[16] Stock K *et al* 2016 Capturing tumor complexity *in vitro*: comparative analysis of 2D and 3D tumor models for drug discovery *Sci. Rep.* **6** 28951

[17] Xiao W, He J, Nichol J W, Wang L, Hutson C B, Wang B, Du Y, Fan H and Khademhosseini A 2011 Synthesis and characterization of photocrosslinkable gelatin and silk fibroin interpenetrating polymer network hydrogels *Acta Biomater.* **7** 2384–93

[18] Bencherif S A, Srinivasan A, Horkay F, Hollinger J O, Matyjaszewski K and Washburn N R 2008 Influence of the degree of methacrylation on hyaluronic acid hydrogels properties *Biomaterials* **29** 1739–49

[19] Nichol J W, Koshy S T, Bae H, Hwang C M, Yamanlar S and Khademhosseini A 2010 Cell-laden microengineered gelatin methacrylate hydrogels *Biomaterials* **31** 5536–44

[20] Brinkman W T, Nagapudi K, Thomas B S and Chaikof E L 2003 Photo-cross-linking of type I collagen gels in the presence of smooth muscle cells: mechanical properties, cell viability, and function *Biomacromolecules* **4** 890–5

[21] Gaudet I D and Shreiber D I 2012 Characterization of methacrylated type-I collagen as a dynamic, photoactive hydrogel *Biointerphases* **7** 25

[22] Annabi N, Mithieux S M, Zorlutuna P, Camci-Unal G, Weiss A S and Khademhosseini A 2013 Engineered cell-laden human protein-based elastomer *Biomaterials* **34** 5496–505

[23] Koh W-G, Revzin A and Pishko M V 2002 Poly(ethylene glycol) hydrogel microstructures encapsulating living cells *Langmuir* **18** 2459–62

[24] Hutson C B, Nichol J W, Aubin H, Bae H, Yamanlar S, Al-Haque S, Koshy S T and Khademhosseini A 2011 Synthesis and characterization of tunable poly(ethylene glycol): gelatin methacrylate composite hydrogels *Tissue Eng.* A **17** 1713–23

[25] Schukur L, Zorlutuna P, Cha J M, Bae H and Khademhosseini A 2013 Directed differentiation of size-controlled embryoid bodies towards endothelial and cardiac lineages in RGD-modified poly(ethylene glycol) hydrogels *Adv. Healthcare Mater.* **2** 195–205

[26] Sneddon I N 1965 The relation between load and penetration in the axisymmetric boussinesq problem for a punch of arbitrary profile *Int. J. Eng. Sci.* **3** 47–57

[27] Nguyen T D and Gu Y T 2014 Exploration of mechanisms underlying the strain-rate-dependent mechanical property of single chondrocytes *Appl. Phys. Lett.* **104** 1–5

[28] Nguyen T D, Oloyede A, Singh S and Gu Y T 2015 Microscale consolidation analysis of relaxation behavior of single living chondrocytes subjected to varying strain-rates *J. Mech. Behav. Biomed. Mater.* **49** 343–54

[29] Fata J E, Mori H, Ewald A J, Zhang H, Yao E, Werb Z and Bissell M J 2007 The MAPKERK-1, 2 pathway integrates distinct and antagonistic signals from TGFα and FGF7 in morphogenesis of mouse mammary epithelium *Dev. Biol.* **306** 193–207

[30] Chan V, Zorlutuna P, Jeong J H, Kong H and Bashir R 2010 Three-dimensional photopatterning of hydrogels using stereolithography for long-term cell encapsulation *Lab Chip* **10** 2062–70

[31] Bhadriraju K and Chen C S 2002 Engineering cellular microenvironments to improve cell-based drug testing *Drug Discovery Today* **7** 612–20

[32] Birgersdotter A, Sandberg R and Ernberg I 2005 Gene expression perturbation *in vitro*—a growing case for three-dimensional (3D) culture systems *Semin. Cancer Biol.* **15** 405–12

[33] Breslin S and O'Driscoll L 2013 Three-dimensional cell culture: the missing link in drug discovery *Drug Discovery Today* **18** 240–9

[34] Imamura Y *et al* 2015 Comparison of 2D- and 3D-culture models as drug-testing platforms in breast cancer *Oncol. Rep.* **33** 1837–43

[35] Bissell M J, Kenny P A and Radisky D C 2005 Microenvironmental regulators of tissue structure and function also regulate tumor induction and progression: the role of extracellular matrix and its degrading enzymes *Cold Spring Harb. Symp. Quant. Biol.* **70** 343–56

[36] Neve R M *et al* 2006 A collection of breast cancer cell lines for the study of functionally distinct cancer subtypes *Cancer Cell* **10** 515–27

[37] Kenny P A *et al* 2007 The morphologies of breast cancer cell lines in three-dimensional assays correlate with their profiles of gene expression *Mol. Oncol.* **1** 84–96

[38] Pickl M and Ries C H 2009 Comparison of 3D and 2D tumor models reveals enhanced HER2 activation in 3D associated with an increased response to trastuzumab *Oncogene* **28** 461–8

[39] Pampaloni F, Reynaud E G and Stelzer E H 2007 The third dimension bridges the gap between cell culture and live tissue *Nat. Rev. Mol. Cell Biol.* **8** 839–45

[40] Kim S H, Lee G H and Park J Y 2013 Microwell fabrication methods and applications for cellular studies *Biomed. Eng. Lett.* **3** 131–7

[41] Kang A, Seo H I, Chung B G and Lee S H 2015 Concave microwell array-mediated three-dimensional tumor model for screening anticancer drug-loaded nanoparticles *Nanomedicine* **11** 1153–61

[42] Singh M, Close D A, Mukundan S, Johnston P A and Sant S 2015 Production of uniform 3D microtumors in hydrogel microwell arrays for measurement of viability, morphology, and signaling pathway activation *Assay Drug Dev. Technol.* **13** 570–83

[43] Singh M, Mukundan S, Jaramillo M, Oesterreich S and Sant S 2016 Three-dimensional breast cancer models mimic hallmarks of size-induced tumor progression *Cancer Res.* **76** 3732–43

[44] Sage E H 2001 Regulation of interactions between cells and extracellular matrix: a command performance on several stages *J. Clin. Invest.* **107** 781–3

[45] Frantz C, Stewart K M and Weaver V M 2010 The extracellular matrix at a glance *J. Cell. Sci.* **123** 4195–200

[46] Cox T R and Erler J T 2011 Remodeling and homeostasis of the extracellular, matrix: implications for fibrotic diseases and cancer *Dis. Models Mech.* **4** 165–78

[47] Peela N, Sam F S, Christenson W, Truong D, Watson A W, Mouneimne G, Ros R and Nikkhah M 2016 A three dimensional micropatterned tumor model for breast cancer cell migration studies *Biomaterials* **81** 72–83
[48] Foulkes W D, Reis-Filho J S and Narod S A 2010 Tumor size and survival in breast cancer—a reappraisal *Nat. Rev. Clin. Oncol.* **7** 348–53
[49] Lai H W, Kuo S J, Chen L S, Chi C W, Chen S T, Chang T W and Chen D R 2011 Prognostic significance of triple negative breast cancer at tumor size 1 cm and smaller *Eur. J. Surg. Oncol.* **37** 18–24
[50] Thakuri P S, Ham S L, Luker G D and Tavana H 2016 Multiparametric analysis of oncology drug screening with aqueous two phase tumor spheroids *Mol. Pharm.* **13** 3724–35
[51] Schedin P and Keely P J 2011 Mammary gland ECM remodeling, stiffness, and mechanosignaling in normal development and tumor progression *Cold Spring Harb. Perspect. Biol.* **3** a003228
[52] Lu P, Weaver V M and Werb Z 2012 The extracellular matrix: a dynamic niche in cancer progression *J. Cell Biol.* **196** 395–406
[53] Chaudhuri O, Koshy S T, Branco da Cunha C, Shin J W, Verbeke C S, Allison K H and Mooney D J 2014 Extracellular matrix stiffness and composition jointly regulate the induction of malignant phenotypes in mammary epithelium *Nat. Mater.* **13** 970–8
[54] Wozniak M A, Desai R, Solski P A, Der C J and Keely P J 2003 ROCK-generated contractility regulates breast epithelial cell differentiation in response to the physical properties of a three-dimensional collagen matrix *J. Cell Biol.* **163** 583–95
[55] Mason B N, Starchenko A, Williams R M, Bonassar L J and Reinhart-King C A 2013 Tuning 3D collagen matrix stiffness independently of collagen concentration modulates endothelial cell behavior *Acta Biomater.* **9** 4635–44
[56] Barcus C E, Keely P J, Eliceiri K W and Schuler L A 2013 Stiff collagen matrices increase tumorigenic prolactin signaling in breast cancer cells *J. Biol. Chem.* **288** 12722–32